Inorg. Chem. **2005**, *44*, 6082–6091

Comparative Studies of Substitution Reactions of Rhenium(I) Dicarbonyl–Nitrosyl and Tricarbonyl Complexes in Aqueous Media

Niklaus Marti,[†] Bernhard Spingler,[‡] Frank Breher,[§] and Roger Schibli*[,†,§]

Centre for Radiopharmaceutical Science, ETH-PSI-USZ, 5232 Villigen, Switzerland, Department of Chemistry and Applied Biosciences, ETH Zürich, 8093 Zürich, Switzerland, and Institute of Inorganic Chemistry, University of Zürich, 8057 Zürich, Switzerland

Received March 24, 2005

The ligand substitution behavior of $[ReBr_3(CO)_3](NEt_4)_2$ (**1**) and $[ReBr_3(CO)_2(NO)]NEt_4$ (**2**) in aqueous media was compared. Ligand exchange reactions were performed with multidentate chelating systems such as picolylaminediacetic acid (L^1; N,N′,O,O′), nitrilotriacetic acid (L^2; N,O,O′,O″), iminodiacetic acid (L^3; N,O,O′), and bis(2-pyridyl)-methane (L^4; N,N′). The products of the substitution reactions were isolated and characterized by means of IR, NMR, MS, and X-ray structure analysis. NMR and crystallographic analyses confirmed the formation of single structural isomers in all cases with a ligand-to-metal ratio of 1:1. With ligands L^1 and L^2 and precursor **1** the tridentately coordinated complexes $[Re(L^1)(CO)_3]$ (**7**) and $[Re(L^2)(CO)_3]^{2-}$ (**8**) were formed. With precursor **2** the same ligands unexpectedly coordinated tetradentately after displacing a CO ligand, yielding complexes $[Re(L^1)(CO)(NO)]$ (**3**) and $[Re(L^2)(CO)(NO)]^-$ (**4**). In both complexes NO was found to be coordinated trans to the carboxylate group. Time-dependent IR spectra of the reaction of **2** with ligand L^1 and L^2 confirmed the loss of one CO during the reaction. The product of the reaction of **2** with L^3 was identified as the neutral complex $[Re(L^3)(CO)_2(NO)]$ (**5**), again, with the nitrosyl coordinated trans to the carboxylate. With **1**, ligand L^3 formed the anionic complex $[Re(L^3)(CO)_3]^-$ (**9**). Finally the reactions with L^4 yielded the complexes $[ReBr(L^4)(CO)_2(NO)]Br$ (**6**) and $[ReBr(L^4)(CO)_3]$ (**10**), in which bromide was found to be coordinated trans to the NO and CO, respectively. The X-ray structures of **3**, **5**–**7**, and **10** are discussed: **3**, monoclinic $P2_1/n$, with $a = 14.607(1)$ Å, $b = 8.057(1)$ Å, $c = 24.721(1)$ Å, $\beta = 107.117(5)°$, and $Z = 4$; **5**, triclinic $P\bar{1}$, with $a = 6.909(1)$ Å, $b = 9.882(1)$ Å, $c = 14.283(1)$ Å, $\alpha = 89.246(9)°$, $\beta = 89.420(9)°$, $\gamma = 86.196(9)°$, and $Z = 4$; **6**, triclinic $P\bar{1}$, with $a = 9.823(1)$ Å, $b = 10.094(1)$ Å, $c = 12.534(1)$ Å, $\alpha = 108.679(9)°$, $\beta = 111.992(9)°$, $\gamma = 95.426(10)°$, and $Z = 2$; **7**, orthorhombic *Pbca*, with $a = 14.567(1)$ Å, $b = 13.145(1)$ Å, $c = 14.865(1)$ Å, and $Z = 8$; **10**, monoclinic $P2_1/c$, with $a = 12.749(1)$ Å, $b = 13.302(1)$ Å, $c = 9.011(1)$ Å, $\beta = 107.195(2)°$, and $Z = 4$.

Introduction

The two radiopharmaceutically relevant isotopes Tc-99m and Re-188 show excellent decay properties for diagnostic (^{99m}Tc, $T_{1/2} = 6$ h; $\gamma = 140$ keV) and therapeutic purposes (^{188}Re, $T_{1/2} = 16.9$ h: $\beta^- = 2.1$ MeV). Both isotopes are readily available as permetallate MO_4^- from a ^{99}Mo/^{99m}Tc or ^{188}W/^{188}Re generator system, respectively.[1] Over the course of the past decade, a growing interest in the chemistry of low-valent rhenium(I) and technetium(I) complexes for application in radiopharmacy has emerged. After the recent development of a simple procedure to obtain *fac*-$[^{99m}Tc(H_2O)_3(CO)_3]^+$ and *fac*-$[^{188}Re(H_2O)_3(CO)_3]^+$, a new class of versatile precursors is now available for potential applications in nuclear medicine.[2,3] Several groups are currently developing suitable and tailor-made ligand systems for the $M(CO)_3$ fragment (M = Tc, Re).[4−11] For the macroscopic syntheses and characterization of corresponding complexes in aqueous media, *fac*-$[ReBr_3(CO)_3]^{2-}$ (anion of **1**), has been recognized nowadays as the synthon of choice.

* Author to whom correspondence should be addressed. E-mail: roger.schibli@psi.ch. Phone: +41-(0)56-310 2837. Fax: +41-(0)56-310 2849.

† Center for Radiopharmaceutical Science.

‡ University of Zürich.

§ ETH Zürich.

(1) Coursey, B. M.; Calhoun, J. M.; Cessna, J.; Hoppes, D. D.; Schima, F. J.; Unterweger, M. P.; Golas, D. B.; Callahan, A. P.; Mirzadeh, S.; Knapp, F. F. *Radioact. Radiochem.* **1990**, 38.

(2) Alberto, R.; Ortner, K.; Wheatley, N.; Schibli, R.; Schubiger, A. P. *J. Am. Chem. Soc.* **2001**, *123*, 3135.

(3) Schibli, R.; Schwarzbach, R.; Alberto, R.; Ortner, K.; Schmalle, H.; Dumas, C.; Egli, A.; Schubiger, P. A. *Bioconjugate Chem.* **2002**, *13*, 750.

10.1021/ic050442h CCC: $30.25
Published on Web 00/00/0000

In the course of in vitro and in vivo experiments it could be shown that major differences of the pharmacological profile of $^{99m}TcL(CO)_3$ complexes (L = mono-, bi-, and tridentate chelate) are dominated and also limited by the denticity and lipophilicity of the chelate L whereas the $M(CO)_3$ fragment is rather "innocent" in this respect. Thus, significant changes in the physicochemical behavior arising from the metal core can only be induced by modification of the $M(CO)_3$ moiety. Thus, we and others set out to investigate the influence of the replacement of one CO ligand within complex **1** with an isolobal nitrosyl group giving rise to a $[M(CO)_2NO]^{2+}$ fragment.[14−16,21] The strong π-acceptor capacities of NO^+ together with the additional positive charge render the metal center "harder" and thus, its preference for chelating system should differ from that of the $[M(CO)_3]^+$ fragment. In addition, nitrosyl ligands exhibit a stronger trans-effect than carbonyl groups. Therefore, ligands located trans to NO^+ are coordinated more tightly to the metal center and hence are less prone to ligand exchange. The increased (substitution) stability of the dicarbonyl−nitrosyl moiety in combination with different chelating systems and biomolecules could potentially lead to new radiopharmaceuticals due to different and/or improved pharmacokinetic properties.

Mixed carbonyl−nitrosyl complexes of $^{185/187}Re$ and ^{99}Tc described in the literature are almost exclusively synthesized in organic solvents.[12−19] However, it is inevitable to develop synthetic pathways in aqueous medium for application in radiopharmacy. Berke and Alberto have described different aspects of the aqueous behavior of *fac*-$[ReX_3(CO)_2(NO)]^-$ (X = Cl, Br, NO_3).[20] Our group has recently developed the synthesis of the precursor *fac*-$[ReBr_3(CO)_2(NO)]^-$ (anion of **2**) and the corresponding radioactive Tc-99m match in aqueous media.[21] We now wish to report the syntheses and comparison of spectroscopic features of a selection of tricarbonyl and dicarbonyl−nitrosyl complexes derived from **2** and **1**.

Experimental Section

All chemicals and solvents used for this investigation were purchased from either Fluka or Sigma-Aldrich and used without further purification unless stated otherwise. THF was dried by distillation from sodium−benzophenone prior to use. Nitrosyl precursor $[ReBr_3(CO)_2(NO)]^-$ (anion of **2**) was prepared from $[ReBr_3(CO)_3]^{2-}$ (anion of **1**) according to procedures previously published.[21] Ligands employed in this study were synthesized by following literature procedures.[22−25] Yields and analytical data (IR, NMR) of synthesized ligands (L^1−L^4) were consistent with those reported in the literature. Sodium salts of L^2 and L^3 were obtained in an aqueous solution from the reaction of the ligands with 3 and 2 equiv of NaOH, respectively. Sep-Pak purifications were carried out with Sep-Pak Vac 20 cm^3 (5 g), 6 cm^3 (1 g), or 1 cm^3 (100 mg) C18 Cartridges purchased from Waters using a H_2O−MeOH gradient. Elution of the products started with pure water, followed by mixtures of H_2O/MeOH (3/1 → 1/1). Pure methanol was used for final elution. Nuclear magnetic resonance spectra were recorded on a 300 MHz Varian Gemini 2000 spectrometer with the corresponding solvent signals as internal standard. Chemical shifts are reported in parts per million (ppm) relative to residual protons of deuterated solvents. Values of coupling constants, *J*, are given in Hertz (Hz). ^2J refers to geminal and ^3J to vicinal proton−proton couplings. The following abbreviations are used in the Experimental Section for the description of ^1H NMR spectra: singlet (s); doublet (d); triplet (t). IR spectra were recorded on a Perkin-Elmer FT-IR 16PC using KBr pellets for solids and an HATR device for aqueous or organic solutions. Mass spectra were measured on an LCT Premier ESI-TOF from Waters, using either the negative or positive ionization mode. ESI-TOF spectra of ligand complexes containing carboxylic acids required measurement in the negative ionization mode because no signals were detected in the positive ionization mode. Elemental analyses of C, H, and N were performed with a LECO CHN-900 from LECO Corp., St. Joseph, MI. Data collection for the X-ray structure determinations were performed on Stoe IPDS (**3**, **5**, and **6**) or Bruker APEX (**7**, **10**) diffractometer systems, respectively, by using graphite monochromated Mo Kα (0.71073 Å) radiation and a low-temperature device. In order to avoid decomposition, the single crystals were mounted in perfluoro ether oil on top of a glass fiber and then brought into the cold nitrogen stream of a low-temperature device so that the oil solidified. All calculations were performed on PCs by using the SHELXS-97[27] and SHELXL-97[28] software packages. All structures were solved by direct methods and successive interpretation of the difference Fourier maps, followed by full matrix least-squares refinement

(4) Allali, M.; Benoist, E.; Habbadi, N.; Gressier, M.; Souizi, A.; Dartiguenave, M. *Tetrahedron* **2004**, *60*, 1167.
(5) Banerjee, S. R.; Babich, J. W.; Zubieta, J. *Inorg. Chem. Commun.* **2004**, *7*, 481.
(6) Banerjee, S. R.; Maresca, K. P.; Francesconi, L.; Valliant, J.; Babich, J. W.; Zubieta, J. *Nucl. Med. Biol.* **2005**, *32*, 1.
(7) Pietzsch, H. J.; Gupta, A.; Reisgys, M.; Drews, A.; Seifert, S.; Syhre, R.; Spies, H.; Alberto, R.; Abram, U.; Schubiger, P. A.; Johannsen, B. *Bioconjugate Chem.* **2000**, *11*, 414.
(8) Saidi, M.; Seifert, S.; Kretzschmar, M.; Bergmann, R.; Pietzsch, H. J. *J. Organomet. Chem.* **2004**, *689*, 4739.
(9) Schibli, R.; La Bella, R.; Alberto, R.; Garcia-Garayoa, E.; Ortner, K.; Abram, U.; Schubiger, P. A. *Bioconjugate Chem.* **2000**, *11*, 345.
(10) Santos, I. G.; Abram, U.; Alberto, R.; Lopez, E. V.; Sanchez, A. *Inorg. Chem.* **2004**, *43*, 1834.
(11) Wei, L. H.; Banerjee, S. R.; Levadala, M. K.; Babich, J.; Zubieta, J. *Inorg. Chim. Acta* **2004**, *357*, 1499.
(12) Hubbard, J. L.; Kimball, K. L.; Burns, R. M.; Sum, V. *Inorg. Chem.* **1992**, *31*, 4224.
(13) Hund, H. U.; Ruppli, U.; Berke, H. *Helv. Chim. Acta* **1993**, *76*, 963.
(14) Rattat, D.; Schubiger, P. A.; Berke, H. G.; Schmalle, H.; Alberto, R. *Cancer Biother. Radiopharm.* **2001**, *16*, 339.
(15) Rattat, D.; Verbruggen, A.; Berke, H.; Alberto, R. *J. Organomet. Chem.* **2004**, *689*, 4833.
(16) Rattat, D.; Verbruggen, A.; Schmalle, H.; Berke, H.; Alberto, R. *Tetrahedron Lett.* **2004**, *45*, 4089.
(17) Tam, W.; Lin, G. Y.; Wong, W. K.; Kiel, W. A.; Wong, V. K.; Gladysz, J. A. *J. Am. Chem. Soc.* **1982**, *104*, 141.
(18) Veghini, D.; Berke, H. *Inorg. Chem.* **1996**, *35*, 4770.
(19) Veghini, D.; Nefedov, S. E.; Schmalle, H.; Berke, H. *J. Organomet. Chem.* **1996**, *526*, 117.
(20) Kurz, P.; Rattat, D.; Angst, D.; Schmalle, H.; Spingler, B.; Alberto, R.; Berke, H.; Beck, W. *Dalton Trans.* **2005**, 804.
(21) Schibli, R.; Marti, N.; Maurer, P.; Spingler, B.; Lehaire, M. L.; Gramlich, V.; Barnes, C. L. *Inorg. Chem.* **2005**, *44*, 683.
(22) Sperber, N.; Papa, D.; Schwenk, E.; Sherlock, M. *J. Am. Chem. Soc.* **1951**, *73*, 3856.
(23) Newkome, G. R.; Joo, Y. J.; Evans, D. W.; Pappalardo, S.; Fronczek, F. R. *J. Org. Chem.* **1988**, *53*, 786.
(24) Abbotto, A.; Bradamante, S.; Pagani, G. A.; Rzepa, H.; Stoppa, F. *Heterocycles* **1995**, *40*, 757.
(25) Alberto, R.; Schibli, R.; Egli, A.; Schubiger, A. P.; Abram, U.; Kaden, T. A. *J. Am. Chem. Soc.* **1998**, *120*, 7987.
(26) *STOE-IPDS Software package*, 2.87; STOE & Cie, GmbH: Darmstadt, Germany, 1998.
(27) Sheldrick, G. M. *SHELXL97-2: Program for the Refinement of Crystal Structures*; University Göttingen: Göttingen, Germany, 1997.
(28) Altomare, A.; Burla, M. C.; Camalli, M.; Cascarano, G. L.; Giacovazzo, C.; Guagliardi, A.; Moliterni, A. G. G.; Polidori, G.; Spagna, R. *J. Appl. Crystallogr.* **1999**, *32*, 115.

(against F^2). The collected intensities were corrected for Lorentz and polarization factors, and an absorption correction (numerical: **3**, **5**, and **6**; empirical: **7**, **10** (SADABS, version 2.03)) was applied. All atoms were refined anisotropically, except for three carbon atoms in **7**, which had to be refined using the ISOR restraint. The contribution of the hydrogen atoms, in their calculated positions, was included in the refinement using a riding model. The carboxyl hydrogen atom in **7** could be located in a Fourier difference density map but was restrained to an ideal position during refinement, using the implemented HFIX riding model. Upon convergence, the final Fourier difference map of the X-ray structures showed no significant peaks. For **7** and **10**, some residual electron density was located close to the heavy atom rhenium (~0.9−1 Å). Relevant data concerning crystallographic data, data collection, and refinement details are compiled in Table 1. Crystallographic data (excluding structure factors) for the structures reported in this paper have been deposited with the Cambridge Crystallographic Data Centre as supplementary publications CCDC 281452−281456. Copies of the data can be obtained free of charge on application to CCDC, 12 Union Road, Cambridge CB2 1EZ, U.K. (Fax: (+44) 1223-336-033. E-mail: deposit@ccdc.cam.ac.uk. Internet: www.ccdc.cam.ac.uk/conts/retrieving.html. ORTEP plots were drawn with the program ORTEP-3 for Windows at a probability of 50%.[29]

Synthesis of [Re(L^1)(CO)(NO)] (3). 25 mg (0.039 mmol) of precursor **2** were dissolved in 3.5 mL of MeOH/H_2O (2/1). After addition of 8.8 mg (0.039 mmol) of picolylaminediacetic acid, the mixture was stirred at 75 °C for 20 h. The resulting solution was purified by chromatography on a Sep-Pak column, first eluting with H_2O and then H_2O/MeOH (3/1), H_2O/MeOH (1/1), and finally MeOH. The fractions containing the product were evaporated under reduced pressure, and the residue was recrystallized from H_2O/MeOH yielding **3** as a yellow solid (15.8 mg, 72.4%). ^{1}H NMR (D_2O; δ): 9.03 (d, 1H, J = 6 Hz); 8.23 (t, 1H, J = 7.5 Hz); 7.85 (d, 1H, J = 7.5 Hz); 7.61 (t, 1H, J = 6 Hz); 5.35 (d, 1H, J = 15 Hz); 4.91 (d, 1H, J = 15 Hz); 4.61 (d, 1H, J = 16 Hz); 4.43 (d, 1H, J = 16 Hz); 4.13 (d, 1H, J = 18 Hz); 4.04 (d, 1H, J = 18 Hz). ^{13}C NMR (DMSO-d_6; δ): 212.3; 179.6; 179.2; 160.4; 158.5; 142.1; 127.6; 125.3; 69.8; 66.2 (CH_2); 61.4 (CH_2). IR (KBr; cm^{-1}): 1992 (s, ν_{CO}); 1720 (s, ν_{NO}); 1680 (s, ν_{COO}). TOF MS (ES$^-$; m/z): 465.88, 463.89; calcd for $C_{11}H_9N_3O_6{}^{185/187}$Re, [M − 1] = 466.0, 464.0. Anal. Calcd for $C_{11}H_{10}N_3O_6$Re: C, 28.33; H, 2.16; N, 9.01. Found: C, 28.74; H, 2.79; N, 9.51.

Synthesis of NEt$_4$[Re(L^2)(CO)(NO)] (4). To a solution of 20 mg (0.031 mmol) of **2** in 1.5 mL of H_2O/MeOH (1/2) was added 8 mg of trisodium nitrilotriacetate (0.031 mmol), and the solution was stirred at 80 °C for 19 h. The reaction solution was purified with a Sep-Pak column. The product fractions were combined and dried under N_2. The residue was extracted with acetone, and the filtrate was evaporated under reduced pressure to yield **4** as a yellow powder (7.9 mg, 58.6%). ^{1}H NMR (CD_3OD; δ): 4.3 (d, 1H, J = 17 Hz); 4.26 (d, 1H, J = 17 Hz); 4.08 (d, 1H, J = 17 Hz); 4.02 (d, 1H, J = 17 Hz); 3.99 (d, 1H, J = 17 Hz); 3.9 (d, 1H, J = 17 Hz). ^{13}C NMR (CD_3OD; δ): 211.39; 207.13; 184.98; 182.95; 174.17; 71.60; 65.97; 64.85. IR (KBr; cm^{-1}): 1999 (m); 1735 (m); 1654 (s). TOF MS (ES$^-$; m/z): 432.95, 430.95 (calcd for $C_7H_6N_2O_8{}^{185/187}$Re, [M] = 432.96, 430.96).

Synthesis of [Re(L^3)(CO)$_2$(NO)] (5). 20 mg (0.031 mmol) of precursor **2** were dissolved in 1.5 mL of H_2O/MeOH (1/2), and 5.6 mg (0.032 mmol) of disodium iminodiacetate was added. The yellow solution was stirred at 80 °C for 20 h. The volume of the reaction solution was reduced under vacuum and the product purified with a Sep-Pak column. The fractions containing the product were dried under reduced pressure. The residue was extracted with CH_2Cl_2 to yield, after evaporation under reduced pressure, **5** as a yellow powder (11.4 mg, 90.8%). Crystals suitable for X-ray analysis were grown from a CH_2Cl_2 solution upon slow evaporation of the solvent. ^{1}H NMR (DMSO-d_6; δ): 7.83 (t, 1H, ^3J = 7 Hz); 4.04 (dd, 1H, ^3J = 7 Hz, ^2J = 17 Hz); 3.88 (dd, 1H, ^3J = 7 Hz, ^2J = 17 Hz); 3.69 (d, 1H, ^2J = 17 Hz); 3.68 (d, 1H, ^2J = 17 Hz). ^{13}C NMR (DMSO-d_6; δ): 189.7; 189.4; 179.4; 178.9; 55.0; 54.6 ppm. IR (KBr; cm^{-1}): 2099 (s); 2027 (s); 1762 (s); 1698 (s). TOF MS (ES$^-$; m/z): 402.94, 400.93 (calcd for $C_6H_4N_2O_7{}^{185/187}$Re, [M − 1] = 402.95, 400.95). Anal. Calcd for $C_6H_5N_2O_7$Re: C, 17.87; H, 1.25; N, 6.95. Found: C, 17.80; H, 1.29; N, 6.68.

Synthesis of [ReBr(L^4)(CO)$_2$(NO)]Br (6). Method A. After 30 mg (0.047 mmol) of precursor **2** was dissolved in 3 mL of H_2O/MeOH (5/1), a solution of 8.1 mg of L^4 (0.047 mmol) in 0.9 mL of H_2O/MeOH (1/1) was added. The mixture was stirred at 75 °C for 16 h. Then, 7.6 mg (0.039 mmol) of $AgBF_4$ was added to the solution and stirring was continued at room temperature for 1 h. The white precipitate was filtered off, and the filtrate was concentrated under reduced pressure. The residual product was washed first with dry THF and then extracted with acetone to remove the remaining NEt_4Br salt. Filtration yielded **6** as a yellow powder (26 mg, 92.4%).

Method B. 16 mg (0.031 mmol) of **10** were dissolved in 2 mL of CH_2Cl_2, and 7 mg (0.059 mmol) of $NOBF_4$ was added. The solution was stirred at room temperature for 16 h, and the solvent was removed under reduced pressure. The residue was precipitated from MeOH/Et_2O to yield **6** as a yellow powder (11 mg, 58.7%). ^{1}H NMR (CD_3Cl; δ): 9.06 (d, 2H, J = 6 Hz); 8.83 (d, 2H, J = 8 Hz); 8.18 (t, 2H, J = 7 Hz); 7.57 (t, 2H, J = 6 Hz); 6.36 (d, 1H, J = 16.5 Hz); 4.44 (d, 1H, J = 16.5 Hz). ^{13}C NMR (CD_3Cl; δ): 182.9; 156.4; 155.8; 143.3; 129.3; 126.3; 53.1. IR (KBr; cm^{-1}): 2104 (s); 2048 (s); 1799 (s); 1772 (s). TOF MS (ES$^+$; m/z): 523.93, 521.91, 519.92 (calcd for $C_{13}H_{10}BrN_3O_3{}^{185/187}$Re, [M] = 523.94, 521.94, 519.94). Anal. Calcd for $(C_{13}H_{10}N_3O_3ReBr_2)(C_8H_{20}N)_{1.5}$-$Br_{2.5}$: C, 30.11; H, 4.04; N, 6.32. Found: C, 30.04; H, 4.01; N, 6.35.

Synthesis of [Re(L^1)(CO)$_3$] (7). Complex *fac*-[Re(L^1)(CO)$_3$] (**7**) was prepared according to previously described procedures.[25] To a solution of 55.0 mg (0.071 mmol) of **1** in 5 mL of MeOH was added 23 mg (0.102 mmol) of picolylaminediacetic acid. The solution was stirred at room temperature for 2 h. After evaporation of the solvent under reduced pressure, the residue was washed with CH_2Cl_2 and filtrated. The residue was recrystallized from warm methanol to yield **7** as a white powder (29.1 mg, 82.6%). ^{1}H NMR (DMSO-d_6; δ): 8.76 (d, 1H, J = 5 Hz); 8.14 (t, 1H, J = 8 Hz); 7.86 (d, 1H, J = 8 Hz); 7.58 (t, 1H, J = 7 Hz); 5.13 (d, 1H, J = 16 Hz); 4.73 (d, 1H, J = 16 Hz); 4.54 (d, 1H, J = 17 Hz); 4.3 (d, 1H, J = 17 Hz); 4.05 (d, 1H, J = 17 Hz); 3.64 (d, 1H, J = 17 Hz). ^{13}C NMR (DMSO-d_6; δ): 197.2; 197.1; 196.8; 178.9; 169.9; 159.6; 151.8; 140.5; 125.8; 124.0; 67.8; 67.6; 61.6. IR (KBr; cm^{-1}): 2027 (s); 1916 (s); 1878 (s); 1589 (m). TOF MS (ES$^-$; m/z): 492.82, 490.82 (calcd for $C_{13}H_{10}N_2O_7{}^{185/187}$Re, [M − 1] = 493.0, 491.0). Anal. Calcd for $C_{13}H_{11}N_2O_7$Re: C, 31.64; H, 2.25; N, 5.68. Found: C, 31.42; H, 2.30; N, 5.49.

Synthesis of Na/NEt$_4$[Re(L^2)(CO)$_3$] (8). 10 mg (0.039 mmol) of trisodium nitrilotriacetate were added to a solution of 30 mg (0.039 mmol) of precursor **1** in 2 mL of H_2O. After the solution was stirred at 80 °C for 2.5 h, the solvent was removed under vacuum and the white residue washed with CH_2Cl_2 and $CHCl_3$ to yield **8** as a mixture of Na/NEt_4 salt (17.9 mg, 85.6%). ^{1}H NMR

(29) Farrugia, L. J. *J. Appl. Crystallogr.* **1997**, *30*, 565.

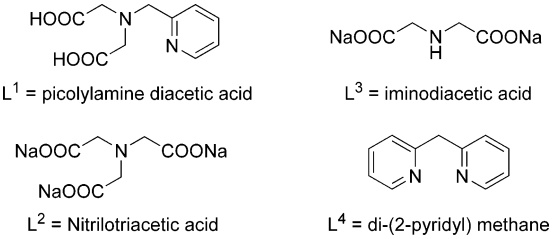

Figure 1. Structures of investigated tetra-, tri-, and bidentate ligand systems.

(CD_3OD; δ): 4.15 (d, 2H, J = 16.5 Hz); 3.65 (d, 2H, J = 16.5 Hz); 3.95 (s, 2H). ^{13}C NMR (CD_3OD; δ): 198.7; 197.9; 183.8; 174.7; 73.4; 64.9; 53.3; 7.6. IR (KBr; cm^{-1}): 2024 (m); 1908 (s); 1889 (s); 1646 (s). TOF MS (ES^-; m/z): 459.78, 457.79 (calcd for $C_9H_6NO_9^{185/187}Re$, [M] = 458.95, 456.95). Anal. Calcd for $(C_9H_6NO_9Re)(C_8H_{20}N)_{0.3}Na_{1.7}$: C, 25.52; H, 2.25; N, 3.39. Found: C, 25.29; H, 2.39; N, 3.51.

Synthesis of $NEt_4[Re(L^3)(CO)_3]$ (9). Method A. To a solution of 12 mg (0.015 mmol) of precursor **1** in 750 μL of CD_3OD was added 2.5 mg (0.014 mmol) of disodium iminodiacetate. The reaction was followed by ^1H NMR spectroscopy at room temperature for 10 min, after which recorded spectra indicated completion of the complexation of the ligand.

Method B. To a solution of 70 mg (0.091 mmol) of complex **1** in 5 mL of EtOH was added 53.6 mg (0.276 mmol) of $AgBF_4$, and the resulting solution was stirred at room temperature for 2 h and filtered. The filtrate was dried under reduced pressure and the residue redissolved in 5 mL of H_2O. Disodium iminodiacetate (16 mg, 0.09 mmol) was added, and the solution was stirred at room temperature for 48 h. The solvent was removed under reduced pressure and the residue extracted with dry THF. The filtrate was dried in vacuo and then precipitated from THF/hexane to yield **9** as a white powder (37.5 mg, 97.3%). ^1H (CD_3OD; δ): 6.44 (t, 1H, ^3J = 7 Hz); 3.58 (dd, 2H, ^3J = 7 Hz, ^2J = 17 Hz); 3.27 (d, 2H, ^2J = 17 Hz). ^{13}C NMR (CD_3OD; δ) 198.1; 183.9; 56.9; 53.2; 7.6. IR (KBr; cm^{-1}): 2025 (s); 1881 (s); 1632 (m). TOF MS (ES^-; m/z): 401.9, 399.91 (calcd for $C_7H_5NO_7^{185/187}Re$, [M] = 401.96, 399.96). Anal. Calcd for $C_{15}H_{25}N_2O_7Re$: C, 33.89; H, 4.74; N, 5.27. Anal. Found: C, 34.10; H, 4.49; N, 5.20.

Synthesis of $[ReBr(L^4)(CO)_3]$ (10). Precursor **1** (30 mg, 0.039 mmol) was dissolved in 500 μL of MeOH, and 6.6 mg (0.039 mmol) of L^4 dissolved in 500 μL of MeOH was added. The solution was stirred at room temperature for 10 min after which the product crystallized. Filtration afforded **10** as white crystals (17.9 mg, 88.4%). ^1H NMR (DMSO-d_6; δ): 9.01 (d, 2H, J = 6 Hz); 8.08 (t, 2H, J = 8 Hz); 7.84 (d, 2H, J = 8 Hz); 7.54 (t, 2H, J = 7 Hz); 4.86 (d, 1H, J = 16 Hz); 4.4 (d, 1H, J = 16 Hz). ^{13}C NMR (DMSO-d_6; δ): 195.8; 156.3; 156.2; 140.6; 125.7; 124.6; 51.4. IR (KBr; cm^{-1}): 2014 (s); 1879 (s). HR-MALDI (m/z): 522, 520, 518 (calcd for $C_{14}H_{10}BrN2O_3^{185/187}Re$, [M] = 521.94, 519.94, 517.94). Anal. Calcd for $C_{14}H_{10}N_2O_3ReBr$: C, 32.32; H, 1.94; N, 5.38. Found: C, 32.45; H, 2.06; N, 5.23.

Results and Discussion

For preliminary studies we focused on the studies of polydentate ligand systems containing carboxylic acids (hard Lewis bases) and aliphatic/aromatic amines (hard/borderline Lewis bases). We compared synthetic and structural features of Re(I) tricarbonyl and mixed carbonyl−nitrosyl complexes with four ligand systems L^1−L^4 (Figure 1).

All Re(I) carbonyl−nitrosyl complexes (Scheme 1) and Re(I) tricarbonyl complexes (Scheme 2) were prepared in aqueous or aqueous−alcoholic solutions with 1 equiv of the corresponding ligand. Under these conditions, both precursors initially formed the corresponding solvated species *fac*-$[Re(sol)_3(CO)_3]^+$ and *fac*-$[ReBr(sol)_2(CO)_2NO]^+$ (sol = solvent), respectively.[21,30] The ligands investigated formed well-defined complexes with **1** and **2** with a metal-to-ligand ratio of 1:1.

In general, we observed, that reactions of precursor **1** with ligands L^1−L^4 were significantly faster accomplished than with **2**, which we partially attribute to the slower bromide and/or water exchange rate observed for **2**.[31] The products could be readily purified by either Sep-Pak columns or extraction into nonpolar organic solvents. All complexes were unambiguously characterized by means of IR, NMR (^1H, ^{13}C, COSY), and mass spectroscopy. Structures of complexes $[Re(L^1)(CO)(NO)]$ (**3**), $[Re(L^3)(CO)_2(NO)]$ (**5**), $[ReBr(L^4)(CO)_2(NO)]Br$ (**6**), $[Re(L^1)(CO)_3]$ (**7**), and $[ReBr(L^4)(CO)_3]$ (**10**) could be elucidated by X-ray diffraction. Data for X-ray analyses are listed in Table 1. To clarify the assignment of individual NMR signals, we used the atom-numbering as shown in the ORTEP plots of the corresponding complexes (Figures 4, 8, and 9).

Substitution Reactions with Ligand L^1: Synthesis of Complexes 3 and 7. Picolylaminediacetic acid (L^1) has been previously investigated with synthon *fac*-$[^{99}TcCl_3(CO)_3]^{2-}$.[25] Reaction of ligand L^1 with **1** was completed in MeOH at room temperature after 2 h yielding complex **7** (83%). In contrast, the reaction of L^1 with precursor **2** was completed only after 20 h at 75 °C affording product **3** in equally good yields (72%). The IR spectra of product **7** displayed the expected facial $M(CO)_3$ pattern (2027, 1916, and 1878 cm^{-1}). To our surprise, after workup of the reaction between **2** and L^1 only one ν(CO) band (1994 cm^{-1}) was detected and the ν(NO) band was found red-shifted at 1719 cm^{-1} (compared to 1753 cm^{-1} in case of **2**). Obviously one CO ligand was cleaved from the Re(I) center during the reaction with L^1 although no evolution of CO could be observed. Figure 2 depicts the time-dependent IR spectra in the region between 2200 and 1500 cm^{-1}. Spectrum A depicts the reaction after 5 min, revealing almost exclusively absorptions of the starting material (∗) together with an intermediate product (#). Spectrum B, recorded after 1 h at 75 °C, shows the disappearance of the starting material and the growing signals of an intermediate as well as the appearance of the final tetradentate-coordinated product $[Re(L^1)(CO)(NO)]$ (**3**) ($). After 4 h at 75 °C the peaks of starting material and intermediate product had further faded (Figure 2C). Spectrum D of complex **3** was observed after 20 h (Figure 2D).

^1H NMR of the free ligand L^1 displays three methylene groups appearing as two singlets (4.59 and 3.86 ppm) with the relative intensity of 1:2. These two singlets disappear

(30) Alberto, R.; Schibli, R.; Egli, A.; Schubiger, P. A.; Herrmann, W. A.; Artus, G.; Abram, U.; Kaden, T. A. *J. Organomet. Chem.* **1995**, *493*, 119.
(31) Grundler, P.; Lehaire, M. L.; Merbach, A.; Schibli, R. Unpublished results.

Scheme 1. Syntheses of the Re(I) Carbonyl-Nitrosyl Complexes[a]

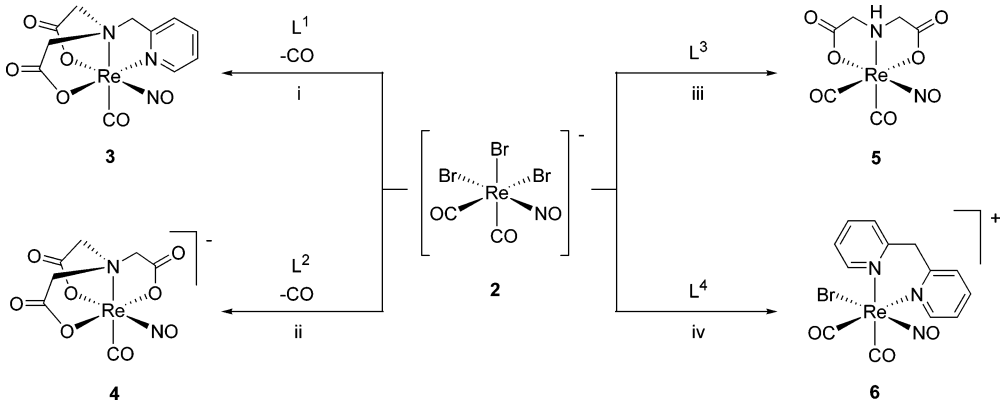

[a] Key: (i) MeOH/H_2O (2/1), L^1 (1 equiv), 75 °C, 20 h; (ii) H_2O/MeOH (1/2), L^2 (1 equiv), 19 h, 80 °C; (iii) H_2O/MeOH (1/2), L^3 (1 equiv), 20 h, 80 °C; (iv) H_2O/MeOH (5/1), L^4 (1 equiv), 16 h, 75 °C.

Scheme 2. Syntheses of the Re Tricarbonyl Complexes[a]

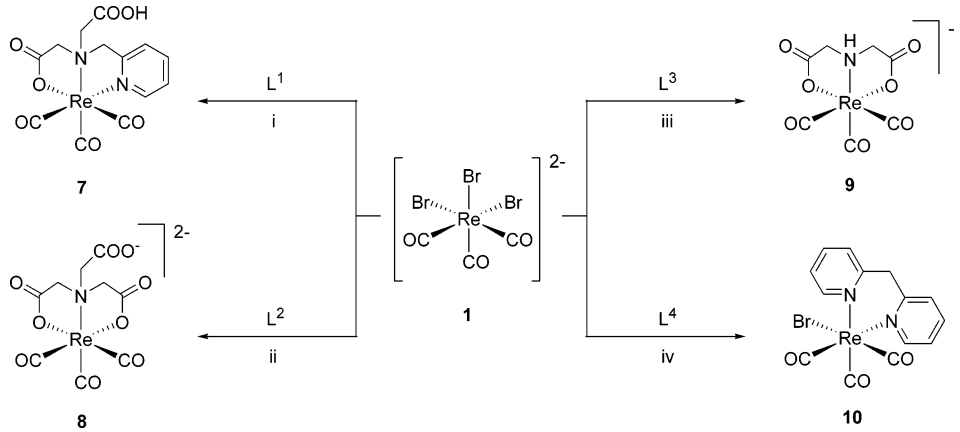

[a] Key: (i) MeOH, L^1 (1.4 equiv), 2 h, RT; (ii) H_2O, L^2 (1 equiv), 2.5 h, 80°; (iii) EtOH, $AgBF_4$ (3 equiv), H_2O, L^3 (1 equiv), 48 h, RT; (iv) MeOH, L^4 (1 equiv), 10 min, RT.

after complexation with **2**, and three pairs of doublets are observed instead (5.35, 4.91, 4.61, 4.43, 4.13, and 4.04 ppm; $J = 15$ Hz, $J = 16$ Hz, and $J = 18$ Hz, respectively). The pattern of the observed three AB spin systems can be explained by the diastereotopic nature of the methylene protons (Figure 3). Similar observations were made with complex **7** (5.13, 4.73, 4.54, 4.3, 4.05, and 3.64 ppm; $J = 16$ Hz, $J = 17$ Hz, and $J = 17$ Hz, respectively) and the corresponding Tc-99 complex.[25] The occurrence of three instead of two AB systems in case of complex **7** could be attributed to a hindered rotation of the noncoordinating acetate group. Interestingly, this third AB system did not collapse to form a singlet even at higher temperatures (DMSO-d_6, 120 °C). A low-field shift of the aromatic peaks compared to the free ligand could be observed in both complexes **3** and **7**.

Crystals of X-ray quality of **3** were obtained by diffusion of MeOH into an aqueous solution of the complex, whereas **7** crystallized from MeOH upon evaporation of the solvent. Selected bond lengths and angles of **3** and **7** are given in Table 2. The X-ray analyses of **3** corroborated the spectroscopically anticipated structure of a monocarbonyl−mononitrosyl complex with the ligand coordinated tetradentately in a pseudo "umbrella-like" fashion (Figure 4A). The NO^+ ligand of **3** is coordinated trans to a carboxylate group, and the second carboxylate is located trans to the pyridine nitrogen. The ternary amine is coordinated trans to the remaining CO ligand within **3**.

Complex **3** possesses a strongly distorted octahedral coordination environment. These deformations are caused by the restraints imposed by the skeleton of the ligand. This is evident from the tilted angles C1−Re1−N2 (167.5°) and O3−Re1−N3 (157.9°). Also, the angles Re1−N3−C11 and Re1−N3−C7 (127.6 and 113.1°) of the five-membered ring formed by the ligand and the metal center show steric strains. The Re1−C1 bond length was found to be 1.94 Å and the Re1−N1 bond was determined as 1.781 Å, enabling unambiguously the assignment of the NO^+ or CO group, respectively. The N−O bond length (1.193 Å) and C−O distance (1.151 Å) are significantly different. The Re1−O5 distance of 2.025 Å trans to the NO^+ is significantly shorter than the Re1−O3 distance of 2.105 Å trans to the pyridine ring, which can be explained by the strong trans-influence of NO^+.

In complex **7**, ligand L^1 coordinates tridentately via the two amines and one carboxylate group. The same coordination has been reported for the corresponding Tc-99 complex.[25] The coordination sphere of Re(I) in **7** was also found to be distorted. However, the corresponding angles C13−Re1−N1 (174.7°) and C11−Re1−N2 (170.9°) are

Table 1. Crystal Data for Compounds **3**, **5**−**7**, and **10**

param	**3**	**5**	**6**	**7**	**10**
formula	$C_{23}H_{24}N_6O_{13}Re_2$	$C_6H_5N_2O_7Re$	$C_{13}H_{10}N_3O_3Br_2Re$	$C_{13}H_{11}N_2O_7Re$	$C_{14}H_{10}N_2O_3BrRe$
fw	964.88	403.32	602.25	493.44	520.36
temp (K)	183(2)	183(2)	183(2)	200(2)	200(2)
cryst syst	monoclinic	triclinic	triclinic	orthorhombic	monoclinic
space group	$P2_1/n$	$P\bar{1}$	$P\bar{1}$	*Pbca*	$P2_1/c$
a, Å	14.607(1)	6.909(1)	9.823(1)	14.567(1)	12.749(1)
b, Å	8.057(1)	9.882(1)	10.094(1)	13.145(1)	13.302(1)
c, Å	24.721(1)	14.283(1)	12.534(1)	14.865(1)	9.011(1)
α (deg)		89.246(9)	108.679(9)		
β (deg)	107.117(5)	89.420(9)	111.992(9)		107.195(2)
γ (deg)		86.196(9)	95.426(10)		
V (Å^3)	2780.6(2)	973.01(12)	1058.82(15)	2846.4(4)	1459.8(2)
Z	4	4	2	8	4
D_c (g/cm^3)	2.31	2.75	2.13	2.303	2.37
μ (mm^{-1})	8.78	12.51	9.54	8.579	11.07
cryst dimens (mm)	0.33 × 0.28 × 0.11	0.13 × 0.08 × 0.03	0.29 × 0.22 × 0.18	0.20 × 0.08 × 0.06	0.08 × 0.06 × 0.04
F(000)	1832	744	640	1872	968
2θ range (deg)	5.84 ≤ 2θ ≤ 60.84	5.90 ≤ 2θ ≤ 56.56	5.54 ≤ 2θ ≤ 56.56	5.00 ≤ 2θ ≤ 49.42	4.54 ≤ 2θ ≤ 52.74
index range	−20 ≤ *h* ≤ 20	−8 ≤ *h* ≤ 9	−13 ≤ *h* ≤ 13	−17 ≤ *h* ≤ 17	−15 ≤ *h* ≤ 15
	−11 ≤ *k* ≤ 11	−13 ≤ *k* ≤ 13	13 ≤ *k* ≤ 13	−15 ≤ *k* ≤ 15	−16 ≤ *k* ≤ 16
	−35 ≤ *l* ≤ 35	−19 ≤ *l* ≤ 19	−16 ≤ *l* ≤ 16	17 ≤ *l* ≤ 13	11 ≤ *l* ≤ 11
no. of collcd reflcns	58 828	9756	19 274	14 668	12 965
no. of unique reflcns	8302 (R_{int} = 0.0753)	4459 (R_{int} = 0.0404)	4872 (R_{int} = 0.1116)	2431 (R_{int} = 0.0807)	2983 (R_{int} = 0.0458)
no. of params/restraints	399/0	289/0	244/2	209/18	190/0
GOOF on F^2	1.089	0.964	1.097	1.168	1.234
R1/wR2[a] (%)	4.05/11.07	6.76/16.27	7.30/17.36	4.95/9.52	4.46/8.66
max/min residual electron density, e/Å^3	3.847/−3.616	2.253/−1.866	2.410/−1.802	2.263/−2.706	1.560/−1.839

[a] $R1 = \Sigma||F_o| - |F_c||/\Sigma F_o$; $wR2 = \{[\Sigma w(F_o - F_c)^2]/\Sigma wF_o^2]\}^{1/2}$.

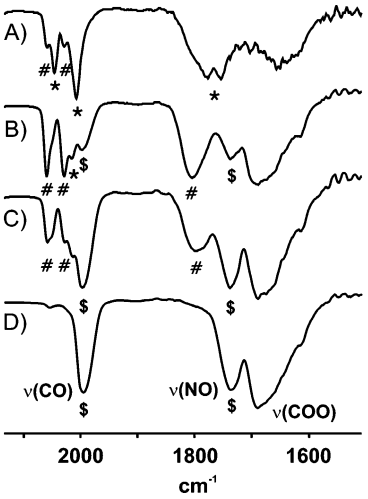

Figure 2. Section of the IR spectra of the reaction of **2** with 1 equiv of L^1 at 75 °C: (A) reaction after 5 min; (B) reaction after 1 h; (C) reaction after 4 h; (D) reaction after 20 h. Absorptions of precursor $[ReBr_3(CO)_2(NO)]^-$ (anion of **2**) are labeled with ∗, and those of the intermediate, with #; the symbol $ represents signals of the final product $[Re(L^1)(CO)(NO)]$ (**3**).

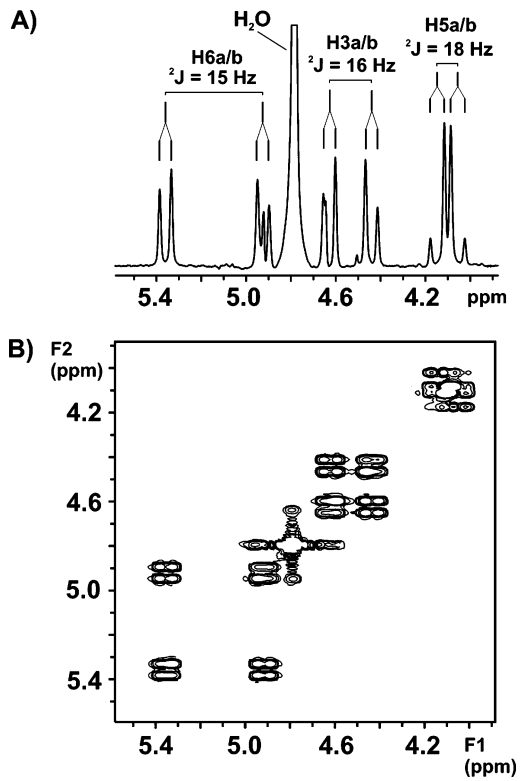

Figure 3. Aliphatic part of the 1D-^{1}H NMR (A) and the COSY spectra of complex **3** (B). Proton labeling corresponds to Figure 4.

closer to 180° than in **3**. The Re−CO bond length trans to the tertiary amine in **7** (1.93 Å) is nearly identical with the corresponding bond observed in **3**. In complex **7**, the bonds Re1−C12 and Re1−C13 are shorter than Re1−C11 due to the different functional groups in trans position.

Complexes **3** and **7** crystallized in both enantiomeric forms (see Supporting Information).

Substitution Reactions with Ligand L^2: Synthesis of Complexes 4 and 8. Experiments with the second tetradentate chelating system L^2 in aqueous medium were performed starting preferentially from the corresponding trisodium salt. Reaction of **2** with L^2 was completed after 19 h at 80 °C yielding, after elution from the Sep-Pak column, approximately 60% of pure product as a mixture of Na/NEt_4 as counterion. As observed for complex **3**, the IR spectrum of product **4** exhibits a monocarbonyl−mononitrosyl pattern (1999, 1735 cm^{-1}). In addition, the analysis of the NMR spectra revealed also in case of ligand L^2 the

Table 2. Bond Lengths (Å) and Angles (deg) of Complexes **3** and **7** with Esd's in Parentheses

[Re(L^1)(CO)(NO)] (**3**)		[Re(L^1)(CO)$_3$] (**7**)	
Re(1)−N(1)	1.781(5)	Re(1)−C(12)	1.90(1)
Re(1)−C(1)	1.941(5)	Re(1)−C(11)	1.93(1)
Re(1)−O(3)	2.105(3)	Re(1)−C(13)	1.90(1)
Re(1)−O(5)	2.025(4)	Re(1)−O(1)	2.132(7)
Re(1)−N(3)	2.118(4)	Re(1)−N(1)	2.132(7)
Re(1)−N(2)	2.159(4)	Re(1)−N(2)	2.241(8)
C(1)−O(1)	1.151(6)	C(11)−O(11)	1.12(1)
C(12)−O(12)	1.09(1)	C(13)−O(13)	1.16(1)
N(1)−O(2)	1.193(1)		
N(1)−Re(1)−C(1)	93.3(2)	C(12)−Re(1)−C(11)	88.9(4)
N(1)−Re(1)−O(5)	179(1)	C(12)−Re(1)−O(1)	171.7(3)
N(1)−Re(1)−O(3)	94.1(1)	C(12)−Re(1)−C(13)	87.2(5)
N(1)−Re(1)−N(3)	93.7(1)	C(12)−Re(1)−N(1)	97.6(4)
N(1)−Re(1)−N(2)	99.2(1)	C(12)−Re(1)−N(2)	93.5(4)
C(1)−Re(1)−N(2)	167.5(2)	C(11)−Re(1)−N(2)	170.9(4)
O(1)−C(1)−Re(1)	175.6(5)	O(11)−C(11)−Re(1)	176.3(9)
O(2)−N(1)−Re(1)	177.8(4)	O(12)−C(12)−Re(1)	176(1)
		O(14)−C(13)−Re(1)	179(1)
C(11)−N(3)−Re(1)	127.6(3)	C(5)−N(1)−Re(1)	126.0(6)
C(7)−N(3)−Re(1)	113.1(3)	C(1)−N(1)−Re(1)	115.9(7)

formation of a single isomer. ^{1}H NMR data for **4** showed three overlapping pairs of doublets with the relative proton intensities 2:2:2 representing three AB-spin systems with coupling constants similar to those observed for complex **3** (J = 17 Hz).

Reaction of **1** with ligand L^2 (2.5 h, 80°) yielded the tridentately coordinated complex **8** (86%). No decarbonylation was observed, even if the reaction was performed at elevated temperature. Proton NMR of complex **8** shows a single AB-spin system (4 H) and one singlet (2 H), due to the C_s symmetry of complex **8**. Unlike observed for complex **7**, the protons of the noncoordinating acetate group appeared as a singlet indicating less hindrance of the rotation around the N−C bond in case of complex **8**.

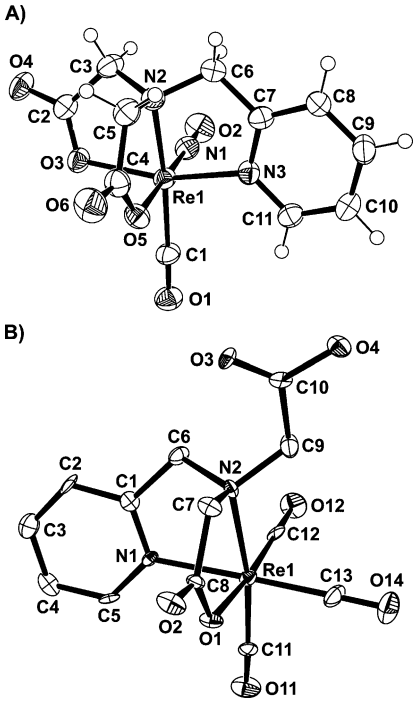

Figure 4. ORTEP plot of the neutral complexes (A) [Re(L^1)(CO)(NO)] (**3**) and (B) [Re(L^1)(CO)$_3$] (**7**). Atoms are drawn at 50% probability.

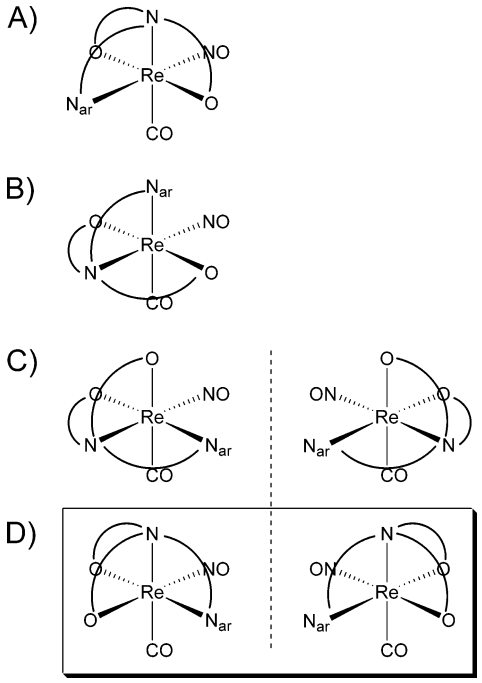

Figure 5. Schematic drawing of possible structural isomers with the composition [Re(L^1)(CO)(NO)]. (D) represents the isomer found by X-ray analysis.

Complexation of ligand L^1 and L^2 (and L^3) with **2** could potentially lead to the formation of structural isomers with a facial and cis configuration, respectively, of the π-acceptor ligands (Figure 5). However, as mentioned above IR, NMR, and X-ray analyses show clear evidence that only one of the possible isomers was formed (Figure 5D). Hence, the following structural preferences can be derived: (i) It is unlikely that the two carboxyl groups are coordinated in a trans position (Figure 5A,B) but rather cis as reported for octahedral Cu(II) or V(IV/V) complexes with L^1.[32,33] (ii) Coordination of carboxylate occurs preferentially in the trans-position to NO$^+$ (Figure 5D).

The formation of single structural isomers in case of complexes **3** and **4** can presumably be explained best by the selective dissociation of the metal-coordinated halides and a preference for strong σ-donor trans to NO$^+$. The halide ligands of **2** coordinated trans to the carbonyl groups are more rapidly exchanged with H_2O in aqueous solution, whereas the third halide ligand trans to the nitrosyl group is more resistant toward substitution.[20,21] Presumably, ligands L^1 and L^2 temporarily coordinate bidentately via the tertiary amine and the pyridine (L^1) or one carboxylate group (L^2), replacing two water molecules (Figure 6; intermediate A). This can be concluded from time-dependent NMR experiments, where soon after addition of L^1 to a solution of **2** the signals of the aromatic protons revealed a significant downfield shift due to metal coordination whereas the signal of the acetate protons remained initially unchanged.

(32) Choquesillo-Lazarte, D.; Covelo, B.; Gonzalez-Perez, J. M.; Castineiras, A.; Niclos-Gutierrez, *J. Polyhedron* **2002**, *21*, 1485.
(33) Launay, J. P.; Jeannin, Y.; Daoudi, M. *Inorg. Chem.* **1985**, *24*, 1052.

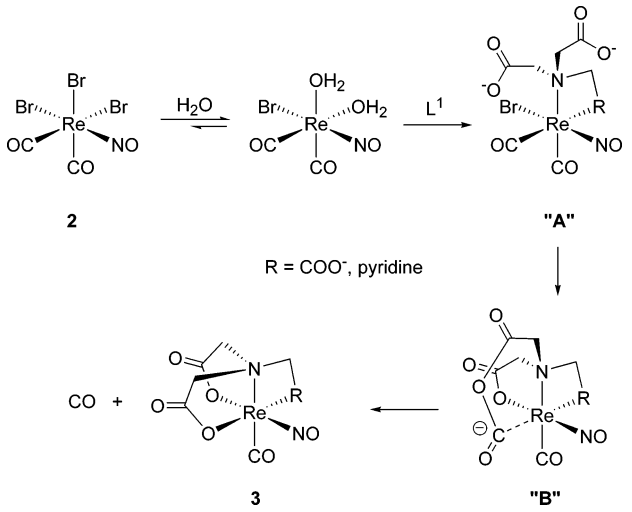

Figure 6. Possible reaction mechanism of the formation of complexes $[Re(L^1)(CO)(NO)]$ (**3**) and $[Re(L^2)(CO)(NO)]^-$ (**4**).

In a third step, one carboxyl group of the chelator displaces the bromide ligand trans to NO^+ (intermediate B). The mechanism of CO displacement remains unclear. It can be speculated that the formation of a "[ReC(O)O(CO)]" species (intermediate B), likely favored by the chelate effect, triggers the cleavage of CO and hence produces the tetradentate complexes **3** and **4**. On the other hand, the solvent seems to play also a decisive role since no decarbonylation and formation of a tetradentate complex was observed during the preparation starting from $[Re(L^2)(CO)_3]^-$ in the presence of $NOBF_4$ in organic solvent.[16]

^{17}O NMR measurements using ^{17}O-enriched H_2O and the precursor $[Re(H_2O)_3(CO)_2NO]^{2+}$ revealed a fast exchange of $M(C-^{16}O)$ by ^{17}O.[31] On the other hand, during these experiments the precursor was stable for several days in strong acidic solution without any signs of decarbonylation as for example reported for $[Ru(H_2O)_3(CO)_3]^{2+}$.[34] Therefore, labilization of the M−CO bond is most likely due to the combination of influence of the solvent and denticity of the incoming ligand systems.

Substitution Reactions with Ligand L^3: Synthesis of Complexes 5 and 9. Reaction of **2** with disodium iminodiacetate (L^3) produced the tridentate coordination complex **5** in good yields (91%). The product was purified via Sep-Pak followed by extraction into CH_2Cl_2. The IR spectra of product **5** showed a "blue-shifted" dicarbonyl−mononitrosyl pattern (2099, 2027, 1762 cm^{-1}). No signs of decarbonylation or formation of monocarbonyl−nitrosyl species were observed as evidenced by IR analysis. ^1H NMR revealed again the formation of a single isomer. The occurrence of two distinct AB spin systems could be observed indicating an unsymmetrical coordination of ligand L^2 (coordination of the secondary amine trans to the nitrosyl ligand would result in a C_s symmetry causing a single AB spin system). We postulate that, in the course of the reaction, ligand L^3 initially coordinated bidentately trans to the two CO groups of substrate **2** and subsequently displaced the third bromide trans to the nitrosyl ligand. This is in accordance with the mechanism proposed for L^1 and L^2 (Figure 6).

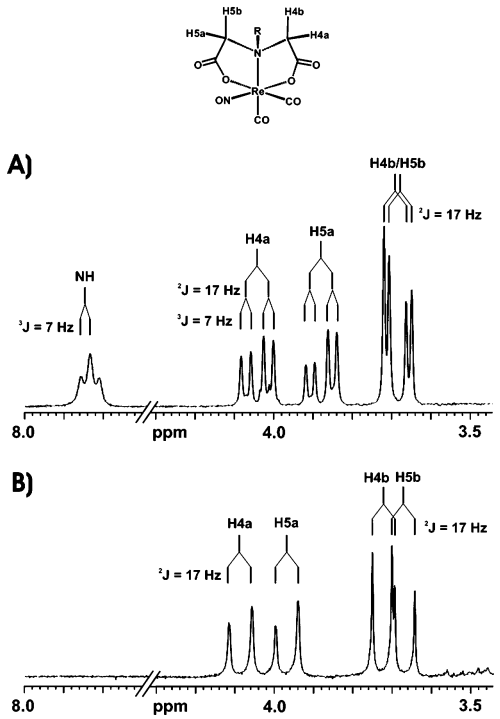

Figure 7. ^1H NMR spectra of complex **5**: (A) spectrum with additional NH-coupling, R = H; (B) spectrum without NH-coupling, R = D. Proton numbering is according to Figure 8.

Directly after a sample was dissolved in CD_3OD, the spectrum of **5** revealed a triplet with the intensity of one proton at 7.83 ppm (J = 7 Hz), which can be assigned to the equatorial NH proton of the secondary amine. The same (additional) coupling constant can be found for the equatorial protons H_{4a} and H_{5a} (Figure 7A). The observed vicinal $^3J(H,H)$ couplings of 7 and 0 Hz, respectively, are in agreement with the Karplus−Conroy curve for $\phi \sim 19°$ ($H_{4a/5a}-C_4-N_2-H_N$) and $\phi \sim 98°$ ($H_{4b/5b}-C_4-N_2-H_N$), respectively.[35,36] The NMR spectrum of the product recorded after 4 h shows two plain AB-spin systems (J_1 and J_2 = 17 Hz) (Figure 7B). The NH peak as well as the additional coupling of the protons H_{4a} and H_{5a} disappeared because of exchange of the NH proton by deuterium (Figure 7B). This indicates a higher acidity of the NH proton of the neutral complex **5** than of the anionic tricarbonyl complex **9** (vide infra).

Reaction of L^3 with precursor **1** in aqueous medium (room temperature, 48 h) yielded the corresponding tricarbonyl complex **9** almost quantitatively (97%). The NMR spectra of complex **9** showed two doublets of an AB-spin system and an additional NH coupling with a coupling constant of 7 Hz. Interestingly, the disappearance of the NH proton over time could not be observed, even after several days in CD_3OD or D_2O. If the synthesis of **9** was performed in CD_3OD/D_2O, the NH coupling was not visible as

(34) Funaioli, T.; Cavazza, C.; Marchetti, F.; Fachinetti, G. *Inorg. Chem.* **1999**, *38*, 3361.
(35) Gutowsky, H. S.; Karplus, M.; Grant, D. M. *J. Chem. Phys.* **1959**, *31*, 1278.
(36) Karplus, M. *J. Am. Chem. Soc.* **1963**, *85*, 2870.

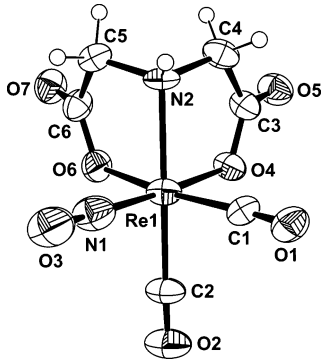

Figure 8. ORTEP plot of complex **5**. Atoms are drawn at 50% probability.

Table 3. Bond Lengths (Å) and Angles (deg) of Complex **5**

Re(1)−N(1)	1.885(9)	Re(1)−N(2)	2.172(7)
Re(1)−C(1)	1.946(9)	C(1)−O(1)	1.11(1)
Re(1)−C(2)	2.01(1)	C(2)−O(2)	1.10(1)
Re(1)−O(4)	2.050(6)	N(1)−O(3)	1.13(1)
Re(1)−O(6)	2.081(6)		
N(1)−Re(1)−C(1)	90.9(4)	N(1)−Re(1)−N(2)	97.8(4)
N(1)−Re(1)−C(2)	90.2(4)	O(1)−C(1)−Re(1)	177.0(8)
C(1)−Re(1)−C(2)	89.7(4)	O(2)−C(2)−Re(1)	178(1)
N(1)−Re(1)−O(4)	176.9(4)	O(3)−N(1)−Re(1)	176(1)
N(1)−Re(1)−O(6)	96.4(4)		

expected, because NH/ND exchange occurred before ligand coordination.

Crystals of **5** suitable for X-ray analysis were grown from a CH_2Cl_2 solution upon slow evaporation of the solvent (Figure 8). The X-ray single-crystal structure of **5** confirmed the spectral analyses. A selection of bond lengths and angles is given in Table 3.

Iminodiacetate (L^3) coordinates tridentately via the two carboxylic acids and the secondary amine. The nitrosyl group in **5** is coordinated trans to the carboxyl group and not trans to the amine again confirming the preference of stronger σ-donors groups trans to NO^+. The Re−N1 (1.885 Å) bond is significantly shorter than the two Re−C bonds (Re1−C1 = 1.946 Å, trans to O6; Re1−C2 = 2.01 Å, trans to N2). The nitrosyl and the carbonyl groups are coordinated almost linearly (176.4−177.7°). However, the angles between the nitrosyl group and the three functional groups of the ligand differ from 90 and 180°, respectively (96.4, 97.8, and 176.9°), showing the steric strain dictated by the two five-membered rings.

Substitution Reactions with Ligand L^4: Synthesis of Complexes 6 and 10. To synthesize the nitrosyl complex **6**, ligand L^4 had to be reacted with precursor **2** at 75 °C for 16 h. Complex **6** was isolated by extraction and analyzed by IR, NMR, and MS. The IR spectra of **6** showed the typical facial $M(CO)_2NO$ pattern (2104, 2048, 1772 cm^{-1}). The aromatic region in the ^1H NMR spectrum evidenced that complexes **6** displays a C_s symmetry. The reaction of precursor **1** with 1 equiv of L^4 directly yielded white crystals of the neutral complex **10**, suitable for X-ray analysis. Spectroscopic data are in agreement with the expected structure.

X-ray analyses proved the proposed structures and compositions (Figure 9). The ligand is coordinated in both complexes trans to the carbonyl groups, whereas the bromide

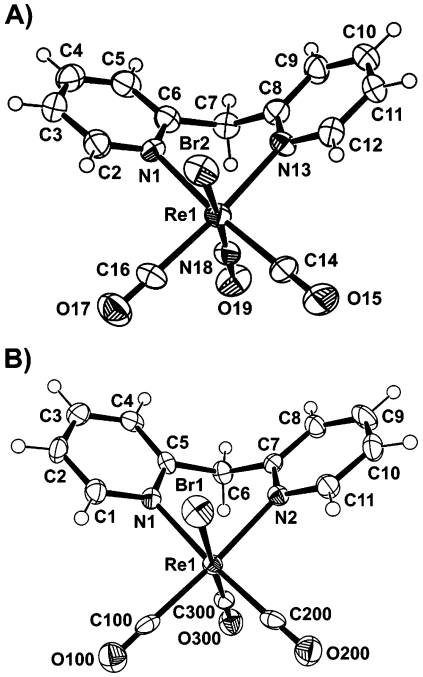

Figure 9. (A) ORTEP plot of complex $[ReBr(L^4)(CO)_2(NO)]Br$ (**6**). The counteranion was omitted for clarity. (B) ORTEP plot of the neutral complex $[ReBr(L^4)(CO)_3]$ (**10**). Atoms are drawn at 50% probability.

Table 4. Bond Lengths (Å) and Angles (deg) of Complexes **6** and **10** with Esd's in Parentheses

$[ReBr(L^4)(CO)_2(NO)]Br$ (**6**)		$[ReBr(L^4)(CO)_3]$ (**10**)	
Re(1)−C(16)	2.018(7)	Re(1)−C(100)	1.98(1)
Re(1)−C(14)	2.030(7)	Re(1)−C(200)	1.949(9)
Re(1)−N(18)	1.784(8)	Re(1)−C(300)	1.880(8)
Re(1)−N(1)	2.198(6)	Re(1)−N(1)	2.192(7)
Re(1)−N(13)	2.179(6)	Re(1)−N(2)	2.198(6)
Re(1)−Br(2)	2.54(1)	Re(1)−Br(1)	2.588(1)
C(16)−O(17)	1.099(9)	C(100)−O(100)	1.05(1)
C(14)−O(15)	1.10(1)	C(200)−O(200)	1.08(1)
N(18)−O(19)	1.17(1)	C(300)−O(300)	1.140(9)
C(14)−Re(1)−N(1)	173.2(3)	C(200)−Re(1)−N(1)	172.9(3)
C(16)−Re(1)−N(13)	173.5(3)	C(100)−Re(1)−N(2)	175.8(3)
N(18)−Re(1)−N(1)	95.6(3)	C(300)−Re(1)−N(1)	96.5(3)
N(18)−Re(1)−N(13)	97.0(3)	C(300)−Re(1)−N(2)	94.1(3)
N(18)−Re(1)−Br(2)	172.6(2)	C(300)−Re(1)−Br(1)	177.9(2)
N(1)−Re(1)−N(13)	83.6(2)	N(1)−Re(1)−N(2)	83.0(2)
C(6)−C(7)−C(8)	114.6(6)	C(5)−C(6)−C(7)	113.3(7)
O(17)−C(16)−Re(1)	179.1(8)	O(100)−C(100)−Re(1)	177.9(8)
O(15)−C(14)−Re(1)	179.3(9)	O(200)−C(200)−Re(1)	177.6(8)
O(19)−N(18)−Re(1)	174.5(6)	O(300)−C(300)−Re(1)	176.3(7)
Re(1)−N(1)−C(6)−C(7)	4(1)	Re(1)−N(1)−C(5)−C(6)	8(1)
Re(1)−N(13)−C(8)−C(7)	0(1)	Re(1)−N(2)−C(7)−C(6)	4(1)

is located trans to the nitrosyl and the third carbonyl group, respectively. Important bond lengths and angles are listed in Table 4.

In complex **6**, the two Re−carbonyl bonds show about the same bond length (2.02 and 2.03 Å, respectively). The bonds are slightly longer than those in complex **10** (1.95 and 1.98 Å). The Re−nitrosyl bond is with 1.78 Å significantly shorter. On the other hand, also the bond Re1−C300 trans to Br1 with 1.88 Å is shorter than the other two Re−C bonds trans to the pyridine nitrogen (1.98 and 1.95 Å). This can be explained by increased π-back-bonding capacity trans to the electron-rich bromide. The octahedral coordination around the Re metal center is slightly more distorted in **6** than in **10** (**6**, C14−Re1−N1 = 173.2°, C16−Re1−N13 =

173.5°, N18−Re1−Br2 = 172.6°; **10**, C200−Re1−N1 = 172.9°, C100−Re1−N2 = 175.8°, C300−Re1−Br1 = 177.9°). The carbonyls in **6** are coordinated almost linearly with 179.1 and 179.3°, whereas the nitrosyl group is slightly bent (174.5°). The three carbonyl groups in **10** are almost linear with 176.3−177.9°. The two aromatic rings form a "butterfly-like" substructure in both complexes. In complex **6**, the Re center almost lies on the intersection of the two planes N1,C6,C7 and N13,C8,C7. The torsion angles Re1−N1−C5−C6 (8°) and Re1−N2−C7−C6 (4°) in **10** are larger than the corresponding angles Re1−N1−C6−C7 (4°) and Re1−N13−C8−C7 (0°) in **6**. The binding angle of the CH_2 group with 114.6°/113.3° (**6**/**10**) is in both complexes slightly stretched compared to the ideal tetrahedral angle.

Conclusion

We have successfully investigated synthetic patterns as well as structural differences and similarities of tricarbonyl and mixed carbonyl−nitrosyl complexes of Re(I) with bi-, tri-, and tetradentate ligand systems in aqueous media. Starting from readily available precursors **1** and **2**, single structural isomers were formed. The coordination preference for strong σ-donors such as a carboxylic group in the trans-position to the nitrosyl resulted in case of precursor **2** in the formation of single isomers. Decarbonylation, yielding monocarbonyl−nitrosyl complexes, was only observed for tetradentate ligands L^1 and L^2 presumably triggered by the denticity of the chelates. However, further investigations with a set of different and structurally diverse tetradentate ligands are yet necessary to support our hypothesis and clarify the observation. All complexes were stable in solution as well as in solid state for several weeks without any signs of decomposition, which is a prerequisite for further development of the corresponding radioactive Tc-99m and Re-188 compounds for potential applications in diagnostic or therapeutic radiopharmacy. In vitro and in vivo experiments with the corresponding radioactive Tc-99m nitrosyl−carbonyl and carbonyl complexes are currently in progress to shed light on their pharmacologic profile.

Acknowledgment. We thank Nihon Medi-Physics for financial support of this work.

Note Added after Print Publication: Incorrect crystallographic data were present in the version posted on the web July 7, 2005 (ASAP) and published in the August 22, 2005 issue (Vol. 44, No. 17, pp 6082−6091); the correct electronic version of the paper was published on September 15, 2005, and an Addition and Correction appears in the October 3, 2005 issue (Vol. 44, No. 20).

Supporting Information Available: X-ray crystallographic data for complexes **3**, **5**−**7**, and **10** in CIF format and ^{1}H and ^{13}C NMR spectra of complexes **3**−**10**. This material is available free of charge via the Internet at http://pubs.acs.org.

IC050442H